Received: 24 February 2020 | Revised: 24 October 2020 | Accepted: 31 October 2020

DOI: 10.1002/ldr.3813

RESEARCH ARTICLE

WILEY

Evaluation of temporal and spatial changes of global ecosystem health

Chen Ran[1,3,5] | Shijie Wang[1,3] | Xiaoyong Bai[1,2,4] | Qiu Tan[5] | Luhua Wu[1,3] | Xuling Luo[1,3,5] | Huan Chen[1,3,5] | Huipeng Xi[1,3] | Qian Lu[1,3]

[1]State Key Laboratory of Environmental Geochemistry, Institute of Geochemistry, Chinese Academy of Sciences, Guiyang, PR China

[2]Center for Excellence in Quaternary Science and Global Change, Chinese Academy of Sciences, Xi'an, PR China

[3]Puding Karst Ecosystem Observation and Research Station, Chinese Academy of Sciences, Puding, PR China

[4]Guizhou Provincial Key Laboratory of Geographic State Monitoring of Watershed, Guizhou Education University, Guiyang, PR China

[5]School of Geography and Environmental Sciences, Guizhou Normal University, Guiyang, PR China

Correspondence
Xiaoyong Bai, State Key Laboratory of Environmental Geochemistry, Institute of Geochemistry, Chinese Academy of Sciences, Guiyang 550081, Guizhou, PR China.
Email: baixiaoyong@vip.skleg.cn

Funding information
The Strategic Priority Research Program of the Chinese Academy of Sciences, Grant/Award Number: XDB40000000 & XDA23060100; National Natural Science Foundation of China, Grant/Award Number: 42077455; United Fund of Karst Science Research Center, Grant/Award Number: U1612441; Western Light Talent Program (Category A), Grant/Award Number: 2018-99

Abstract

Understanding the spatial distribution pattern and driving factors behind ecosystem health is beneficial to ecosystem management and restoration. However, the literature shows little in-depth exploration of regional heterogeneity and the factors that influence ecosystem health on a global scale. This study assesses global ecosystem health for the period 2000–2015 based on the vigor, organization, resilience, and service (VORS) model, and it explores the factors that influence regional differences in ecosystem health. Our results show that: (a) regions with high levels of ecosystem health are distributed mainly near the Equator and within the north–south regression line (0°N–13°N, 0°S–18°S); (b) seven critical zones with high levels of ecosystem health are identified (13°N–18°S, 45°N–65°N, 35°S–56°S, 47°W–80°W, 120°W–130°W, 8°E–37°E, 92°E–157°E); and (c) average annual precipitation and soil moisture play a key role in ecosystem health globally, with correlations of 0.574 and 0.399, respectively. Socioeconomic factors act as bridges, linking and reinforcing the influence of other factors in areas with medium to low levels of ecosystem health. Our study contributes to better understanding of ecosystem health, fills gaps in global ecosystem health diagnosis, and provides reference points for management and recovery of ecosystems.

KEYWORDS

ecosystem health, GDM, influencing factors, regional differences, VORS model

1 | INTRODUCTION

The material basis of life, that is, ecological services needed for the survival and development of human society, are provided by natural ecosystems (Peng, Wang, Wu, Shen, & Pan, 2011). The sustainability of human social development is based on healthy ecosystems (Peng et al., 2011). However, given the rapid development of modern society, intense human activity and the variety of reasonable and unreasonable land use patterns, the structure and functioning of ecosystems have changed greatly (Bingkui, Huilei, Min, & Lu, 2015). Global ecosystem health is showing a downward trend; thus, it is necessary to monitor the health of ecosystems to achieve greater sustainability (Jian, Yanxu, Jiansheng, Huiling, & Xiaoxu, 2015; Rapport & Hildén, 2013).

Scholars have differing concepts of ecosystem health. A healthy ecosystem is resilient to disturbance and does not degenerate over time; its organization and autonomy are resilient to stress (Costanza, 1992a, 1992b; Costanza, Mageau, Norton, & Patten, 1998;

Lu & Li, 2003; Mageau, Costanza, & Ulancowicz, 1995; Rapport, Costanza, & McMichael, 1998). Rapport (1989) was the first to develop the concept of ecosystem health, pointing out that the pursuit of ecosystem health is the basis for sustainable development (Rapport, 2007). Studies related to ecosystem health provide a methodological basis for evaluating the state of the global ecosystem (Rapport et al., 1999), and they confirm that a healthy ecosystem is critical (Costanza, 2012). Costanza's (Costanza & Mageau, 1999) three indicators, namely, ecosystem vigour, ecosystem organization, and ecosystem resilience, constitute the VOR ecosystem health index widely recognized in the ecological community (Ainslie, 1994). Thus far, many ecosystem health assessment studies on various scales have been carried out based on the VOR model. Yan et al. (2016) evaluated ecosystem health in the upstream of the Liaohe River basin based on ecosystem services. Song et al. (2017) used the analytic hierarchy process (AHP) to assess the ecosystem health status of marine life in Laizhou Bay. Yang, Song, and Lu (2020) used a new evaluation framework of pressure, state (vigour-organization-resilience-function), and response to assess the level of land ecosystem health in Qiqihaer City. Rui et al. (Xiao et al., 2019) carried out a comprehensive and detailed analysis of ecosystem health in the eastern coastal metropolitan areas of China; Jian et al. (Jian et al., 2015; Peng, Liu, Li, & Wu, 2017) used Shenzhen and Lijiang, China, to evaluate the health status of urban ecosystems, and found that the contribution of each ecosystem health index to ecosystem health differed at different scales. Wang et al. explored the effects of extreme precipitation on urban ecosystem health (Wang, Deng, Zhou, & Wei, 2018). In addition, there is a body of literature on ecosystem health focusing on single ecosystems that employed methods other than the VOR model (Ishtiaque, Myint, & Wang, 2016; Mariano et al., 2018; Rombouts et al., 2013). Many studies have achieved strong results, which not only yield a better understanding of the ecosystem health at different scales, but also make ecosystem health assessment more accurate by using ecosystem service indicators. However, many studies focus primarily on small regions or river basins, and there is a lack of research on the diagnosis of ecosystem health and its spatial and temporal variation patterns at a global scale. Moreover, the influencing factors affecting ecosystem health remain unclear.

Accordingly, this paper focuses on the global scale and analyzes the spatial and temporal distribution pattern of ecosystem health for the period 2000–2015. The spatial auto-correlation analysis method shows the reliability of this study, confirming that the results are not randomly generated. Finally, this study uses the Spearman correlation analysis model and a geographic detector to understand the individual drivers that contribute most to ecosystem health and the effects from their interactions.

The main objectives of this study are as follows: (a) understanding the spatial and temporal distribution patterns and changes in global ecosystem health and (b) determining the main factors affecting global ecosystem health. Our research extended the assessment of ecosystem health to the global scale, provided a reference for preliminary identification of ecosystem health on a large scale and formed a theoretical basis for balancing socioeconomic development and ecosystem protection.

2 | MATERIALS AND METHODS

2.1 | Data sources and processing

The data required for the spatial quantification of ecosystem health and its influencing factors include land use and NDVI, GIMMS NDVI3g is produced by NASA's Global Inventory Modeling and Mapping Studies (GIMMS) team based on the Advanced Very High Resolution Radiometer (AVHRR) images on NOAA series satellites, which are processed with strict quality control to generate maximum synthetic products (Deng et al., 2019; Tian et al., 2015). The data used for the analysis of the influencing factors of ecosystem health include annual rainfall, temperature, drought index, soil moisture, population density, GDP, etc, the climate dataset are from NOAA climate prediction centre with a horizontal resolution of $0.5^\circ \times 0.5^\circ$ longitude. The remaining required data include global administrative zoning maps and global climate classification data. The specific sources are shown in Table 1.

The data were preprocessed using ARCGIS 10.5 and FRAGSTATS 4.2 software. The landscape indices of ecosystems were calculated using FRAGSTATS 4.2 software. The ecosystem resilience was calculated using ARCGIS 10.5 and ecosystem services were calculated using PYTHON.

2.2 | Methods

2.2.1 | Ecosystem health assessment

Ecosystem health of the spatial entities of an ecosystem, which reflects the ability to maintain healthy structures, to self-regulate, and to recover under stress, can be divided into ecosystem vigour (EV), ecosystem organization (EO), and ecosystem resilience (ER) (Costanza, 1992a, 1992b; Pantus & Dennision, 2005). Therefore, we employ the widely used EHA model, the VOR model proposed by Costanza (1992a, 1992b), then, the indicator of ecosystem services (ES) is added to form a new vigour-organization-resilience-service model (VORS) to evaluate the global ecosystem health. The ecosystem health index (EHI) is expressed as:

$$\mathrm{EHI} = \sqrt[4]{\mathrm{EV} \times \mathrm{EO} \times \mathrm{ER} \times \mathrm{ES}},$$

$$Ai = \frac{Xi - \min Xi}{\max Xi - \min Xi},$$

Where: Ai indicates the dimensionless value of the ith indicator, Xi indicates the actual value of the ith indicator, maxXi represents the maximum value of the ith indicator, minXi represents the minimum value of the ith indicator.

We standardized each indicator to a range of 0–1 based on the range standardization method, and divided the resulting ecosystem health index into five grades according to the equal spacing method (He, Pan, Liu, & Guo, 2019).

TABLE 1 Data sources table

Type of data	Data sources	Website link
Land use type map	Land use/land cover: Dataset from the European Space Agency climate change initiative	https://www.esa-landcover-cci.org/
Normalized Difference Vegetation Index (NDVI)	United States Geological Survey	http://glovis.usgs.gov.cn/
Rainfall data	NOAA Climate Prediction Center	http://www.esrl.noaa.gov/psd/
Temperature data	NOAA Climate Prediction Center	http://www.esrl.noaa.gov/psd/
Index of aridity	European climate assessment & data	http://climexp.knmi.nl/selectfield_obs2.cgi?id=someone@somewhere
Soil moisture	EARTHDATA	https://disc.gsfc.nasa.gov/
Population density	Global human settlements	https://ghslsys.jrc.ec.europa.eu/download.php?ds=pop
Global climate classification data	Koppen's climatic classification	http://koeppen-geiger.vu-wien.ac.at/

Ecosystem vigour can be expressed as ecosystem metabolism or net primary productivity (Rapport et al., 1998). In general, we chose NDVI to represent the indicator of ecosystem vigour (He et al., 2019; Rapport et al., 1998; Wang & Xu, 2017), which has been shown to be effective in many studies related to ecosystem health (Costanza, 2012; Liao et al., 2018; Peng et al., 2017).

Ecosystem organization was obtained based on a landscape pattern index, which reflects the stability of the ecosystem structure (Costanza, 2012; He et al., 2019). We calculate the indexes of landscape heterogeneity (LH), landscape connectivity (LC), and patch connectivity of important ecosystems (IC: forest, water and grassland) to obtain the index of EO (Howell, Muths, Hossack, Sigafus, & Chandler, 2018).

Landscape connectivity represents the overall landscape connectivity to important ecosystems (Cheng, Chen, Sun, & Kong, 2018; Lavorel et al., 2017; Styers, Chappelka, Marzen, & Somers, 2010). Based on existing studies, we weight the three indexes to 0.35, 0.35, and 0.3, respectively, and use the weighted aggregation method to complete the calculation (Frondoni, Mollo, & Capotorti, 2011; Kang, Chen, Hou, & Li, 2018). The equation is as follows:

$$\begin{aligned}EO = {} & 0.35LH + 0.35LC + 0.30IC = 0.25SHDI + 0.10AWMPFD \\ & + 0.25FN_1 + 0.10CONT + 0.07FN_2 + 0.03COHESION_1 \\ & + 0.07FN_3 + 0.03COHESION_2 + 0.07FN_4 + 0.03COHESION_3,\end{aligned}$$

SHDI means shannon diversity index; AWMPFD means fractal dimension index of area-weighted average plaque. FN_1 means landscape fragmentation index; CONTAG means landscape infection index. FN_2, FN_3, FN_4, $COHESION_1$, $COHESION_2$, and $COHESION_3$ respectively forest, water, and grass fragmentation index and patch cohesion index.

A healthy ecosystem is resilient to small disturbances (Rapport et al., 1998). We use the sum of the area-weighted ecosystem resilience coefficients for all the land use types to measure ER and to mitigate the impact of land use on ecosystem resilience (Colding, 2007). Based on expert knowledge and relevant reference materials, the ecosystem resilience coefficient (ERC) is obtained (Jian et al., 2015; Kang et al., 2018; Peng et al., 2017; Tang, Liu, & Zou, 2018). The ecosystem resilience is calculated as follows:

$$ER = \sum_{i=1}^{n} Ai \times ERCi,$$

Where: Ai means the area proportion of land use type *i*; *n* is the number of land use types.

The relative ecosystem service coefficient (RESC) was calculated based on the forest land, and the threshold is [0,1] (Dobbs, Escobedo, & Zipperer, 2011; Jian et al., 2015), as shown in Table 2. In addition, the potential neighbourhoods of land-use types should be considered into the measurement of ecosystem services (Jian et al., 2015; Marulli & Mallarach, 2005). Referring to the existing study, the coefficient of the spatial neighbourhood effect of land use type (CSNE) on ecosystem services is calculated by the coefficient matrix. The calculation formula of ecosystem service is as follows:

$$ES = \sum_{j=1}^{m} RESC_j \times \left(1 + \frac{CSNE_j}{100}\right) \Big/ m,$$

Where: $RESC_j$ is the relative ecosystem service coefficient of the land-use type associated with the pixel *j*; $CSNE_j$ is the sum of the spatial neighbourhood effect coefficients of the four adjacent pixels on the ecosystem service of the pixel *j*; *m* means the pixel evaluate the number of spatial entities.

2.2.2 | Spatial auto-correlation analysis

The significance of spatial auto-correlation analysis is to prove that the aggregation of spatial distribution has a certain rule, not a random distribution. We used this to analyze the clustering pattern of ecosystem health index distribution between regions of the world. Moran's *I* index is used to analyze the spatial agglomeration of the whole

TABLE 2 Table of relative ecosystem service coefficients for each land use type

Land use type	Cultivated land	Forest	Grassland	Wetland	Construction land	Unused land	Water
RESC	0.47	1	0.7	0.93	0.33	0.013	0.85

region (Moran, 1950). The Local Moran's *I* (Anselin, 1995) (LISA) largely reflects the spatial correlation between spatial attribute values and their adjacent spatial attribute values.

$$\text{Moran's } I = \frac{\sum_{i=1}^{n}\sum_{j=1}^{n} Wij(xi-\bar{x})(xj-\bar{x})}{S^2 \sum_{i=1}^{n}\sum_{j=1}^{n} Wij},$$

$$\text{Local Moran's } I = \frac{n(xi-\bar{x})\sum_{j=1}^{m} Wij(xj-\bar{x})}{\sum_{i=1}^{n}(xi-\bar{x})^2},$$

Where: n represents the number of countries in the world, and *m* is the number of countries adjacent to country *j* in space; $i \neq j$, $S = (1/n)\sum_{i=1}^{n}(xi-\bar{x})^2$; x_i, x_j represents ecosystem health value in counties *i* and *j*; *Wij* represents the space weight matrix of unit *i* and *j*; $\bar{x}$ is the average ecosystem health value.

The value of *I* reflects the degree of correlation of the spatial autocorrelation, between −1 and 1. When $I > 0$, there is a positive spatial correlation; when $I < 0$, there is a negative spatial correlation; when $I = 0$, there is no spatial auto-correlation. There are four types of local auto-correlation: high-high (HH), low-low (LL), high-low (HL), and low-high (LH), which means there are a lot of units flock together which have high (or low) level of ecosystem health. A collection of units with high (or low)of ecosystem are surrounded by units with low (or high) ecosystem health value.

2.2.3 | Pearson correlation analysis

For a long time, many scholars have used Pearson correlation analysis to study the relationship between variables (Li et al., 2020; Yang et al., 2019), the determination of the relationship between EHI and influencing factors is mainly accomplished by calculating and verifying the correlation coefficients (Li et al., 2020; Zhang, Feng, Jiang, & Yang, 2015). The formula is presented as follows:

$$R_{xy} = \frac{\sum_{i=1}^{n}\left[(x_i-\bar{X})(y_i-\bar{Y})\right]}{\sqrt{\sum_{i=1}^{n}(x_i-\bar{X})^2 \sum_{i=1}^{n}(y_i-\bar{Y})^2}},$$

Where: n is the number of samples; $\bar{X}$ and $\bar{Y}$ are the means of variables *x* and *y*, respectively; and R_{xy} is the correlation coefficient between variables *x* and *y*. If $|R| \leq .5$, then the correlation between EHI and influencing factors is insignificant; if $|R| \geq .5$, then the correlation coefficients are taken as statistically significant at $p = .05$.

2.2.4 | Geographic detector model

Using the geographic detector model (GDM) (Wang & Xu, 2017), we explored the drivers that influence the health of the global ecosystem and their interactions. This study used a factor detector to measure the impact of influencing factors on ecosystem health. The formula is as follows:

$$q = 1 - \frac{\sum_{h=1}^{L} Nh\sigma_h^2}{N\sigma^2},$$

Where: $h = 1$, and *L* is the stratification of variable *Y* or factor *X*, that is, classification or partitioning. And *Nh* is the number of units in layer *h* and *N* is the whole region respectively; σ_h^2 and σ^2 are respectively the variance of the *Y* value of layer *h* and the whole region. *q* is the explanatory power of independent variables on related variables, the larger the value is, the stronger the explanatory power of independent variables on related variables is, otherwise, the weaker, the range is $0 \sim 1$, and the leading factor of ecosystem health can be identified.

2.2.5 | Statistical analysis

In this paper, we used Data Management Tools (resample) to unify all the data to 0.5° firstly. In order to give an intuitive view of the spatial pattern on global ecosystem health, we use range normalization to standardize the data to 0–1, then, the indexes of ecosystem health were divided into five grades based on the isometric classification: Degraded (0–0.2), Unhealthy (0.2–0.4), Average Health (0.4–0.6), Sub-optimal Health (0.6–0.8), Highest Health (0.8–1.0).

All the figures (Figures 1, 3, and 5) about ecosystem health were designed using ARCGIS 10.5, and the significance of spatial auto-correlation (Figure 5) was to prove that the distribution of global ecosystem health is not a random distribution, but a certain rule. Then based on the spatial analyst tools (Zonal Statistics as Table) to calculated the ecosystem health index for each climate zone, then using ORIGIN LAB 2018 to design Figure 4. Moreover, we calculated the Pearson correlation coefficients between temperature, annual rainfall, drought index, soil moisture, population density, GDP, and ecosystem health, the significance of the correlation was tested using Student's *t* test at $p < .05$ level, R platform was used to design Figure 6, the

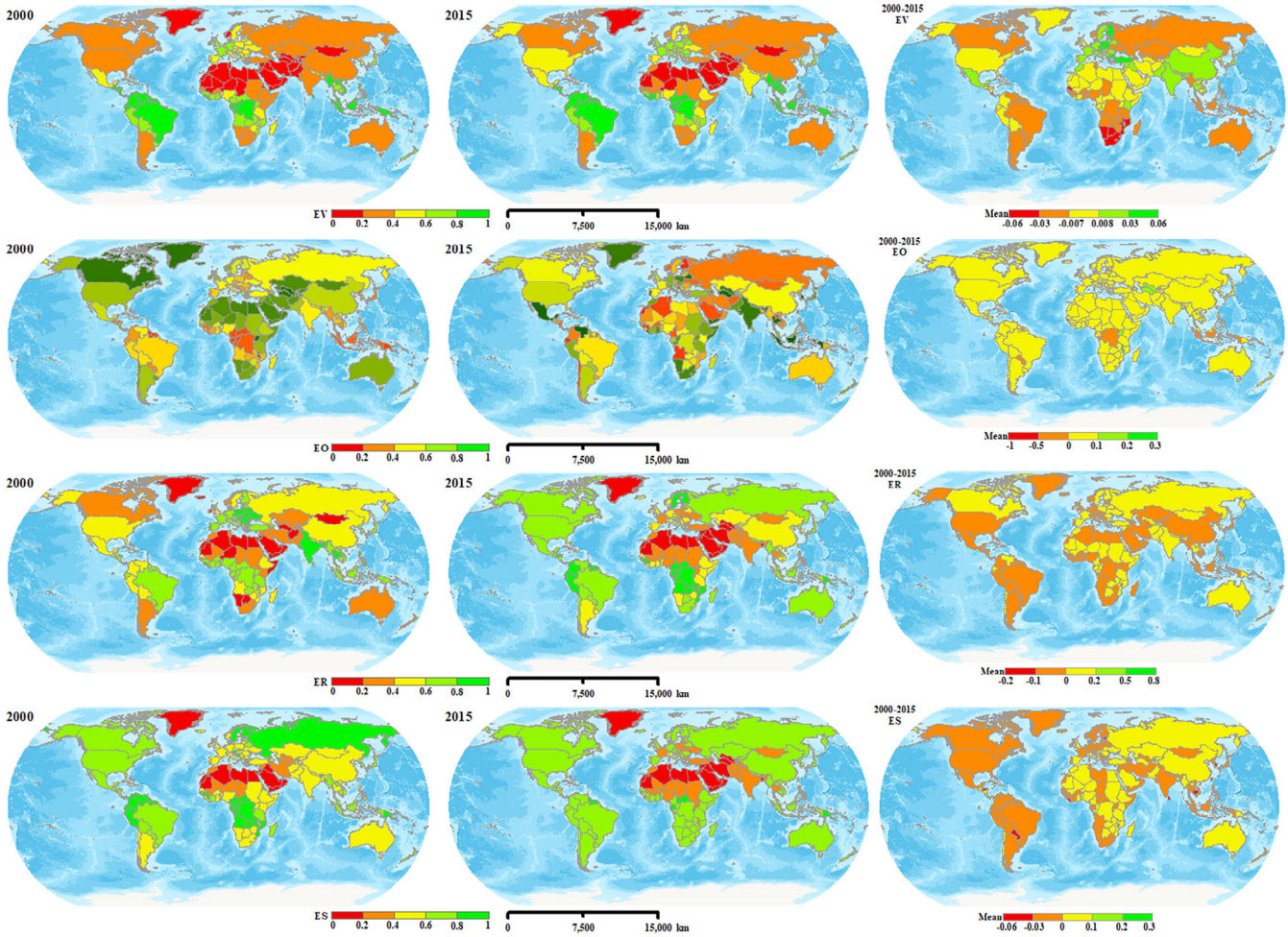

FIGURE 1 The spatial distribution pattern of each ecosystem health indicator [Colour figure can be viewed at wileyonlinelibrary.com]

depth of the colour indicates the degree of correlation between the factors; ORIGIN LAB 2018 was used to design Figure 7.

3 | RESULTS

3.1 | Spatial and temporal distribution pattern of global EHI

We observed the spatial distribution pattern of each ecosystem health indicator from Figure 1. In terms of spatial distribution, high values for global EV are concentrated mainly near the Equator. EV shows a downward trend in Russia, Canada, Australia, Brazil, and other regions over the study period. In Asia, especially in China, there is a significant increasing trend, as India and China have led global vegetation re-greening efforts (Chen et al., 2019). The increase in vegetation cover indicates increasing EV. EO shows an increasing trend on a global scale, and the increase ranges between 0.1 and 0.2. ER shows a decreasing trend in Asia and Europe, with a reduction ranging from 0 to 0.1, which is in contrast to EV; it shows a slight increase in Russia, Canada, and Australia. The spatial distribution of ES shows significant differences, with the Eastern and Western Hemispheres forming a boundary. The Western Hemisphere shows a slight downward trend, and the Eastern Hemisphere shows an increasing trend.

The global spatial distributions of ES and ER show extremely similar patterns. The calculation of both the indicators is based on land use and is largely subject to land use change. In addition, in spatial terms, indicators of ecosystem health show significant differences, and global NDVI is significantly affected by climate factors (Munavar, Carsten, Christian, Dietrich, & Nicole, 2018; Peng, Kuang, & Tao, 2019; Yang et al., 2019; Zheng et al., 2018); as the climate changes, so does the global EV.

From Figure 2, note that the number of countries with higher-than-average health (subhealth and highest health) in 2000, 2005, 2010, and 2015 was 140, 133, 138, and 134, respectively, accounting for 14.92, 14.94, 14.20, and 15% of the total global area. The proportion of healthy countries is almost 50%, but the area is far less than 50%. Similarly, in the same 4 years, the number of countries with below-average health levels (degraded and unhealthy) was 44, 46, 46, and 47, respectively, accounting for 72.13, 71.68, 72.91, and 72.70% of the global total, respectively. Overall, the number of countries above the global average health level has decreased by 4.2% in

the 15-year study period, and the area has shown an N-type change. The proportion of countries with below average health in the world in 2015 increased by 6.8% in number and 0.57% in area compared with 2000.

3.2 | Distribution of average latitude and longitude for average EHI

Combined with the global EHI assessment (Figure 3), the EHIs for 2000, 2005, 2010, and 2015 show very similar spatial distribution patterns. Therefore, we analyze the distribution of the global average EHI from 2000 to 2015 through different longitudinal and latitudinal directions. Seven critical zones are identified. From the perspective of latitude, the distribution of the average health ecosystem index over the study period is mainly along the equator, within the Tropics of Cancer and Capricorn (0°N–13°N, 0°S–18°S). The area with moderate ecosystem health is distributed mainly in the middle latitudes (45°N–65°N, 35°S–56°S). In terms of longitude, the areas with higher ecosystem health are distributed mainly in the Western Hemisphere (47°W–80°W, 120°W–130°W); the Eastern Hemisphere (8°E–37°E, 92°E–157°E) is primarily at the middle ecosystem health level.

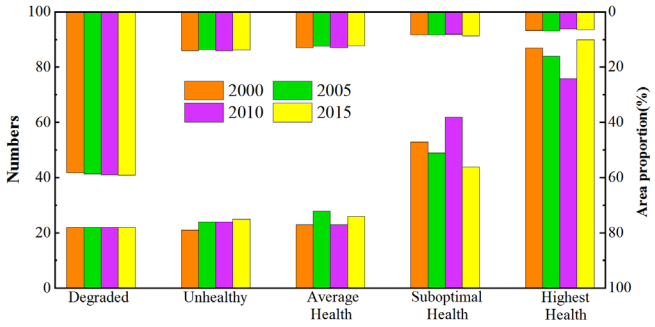

FIGURE 2 Number and area of countries with different levels of ecosystem health index [Colour figure can be viewed at wileyonlinelibrary.com]

3.3 | Distribution of average EHI by climatic zone

Based on the Koppen climatic zone classification, we analyze global distribution of the average EHI from 2000 to 2015. As shown in Figure 4a, this climate classification system was proposed by Wladimir Köppen, a German climatologist. Climatic classification is based on temperature, precipitation, and distribution of natural vegetation. The system divides the world into five climatic zones: tropical (equatorial climatic zone), arid, warm temperate zone, cold temperate zone, and polar climatic zone. Combined with Figure 4b, the global average EHI shows significant differences by climatic zone. The average EHI is 0.49 in the tropics near the Equator, higher than other climatic zones; annual high temperature is elevated, with monthly average temperature above 18°C. In the warm temperate zone, the average EHI is 0.28. The lowest figure is for the polar climatic zone; its average EHI is 0.02. This climatic zone comprises northern Greenland, Antarctica, northeast parts of Siberia, the Qinghai-Tibet Plateau, the Pamirs Plateau, parts of East Africa, and the rocky mountains of the Alps, Andes, and the Chaya Peak of New Guinea, along with other alpine regions

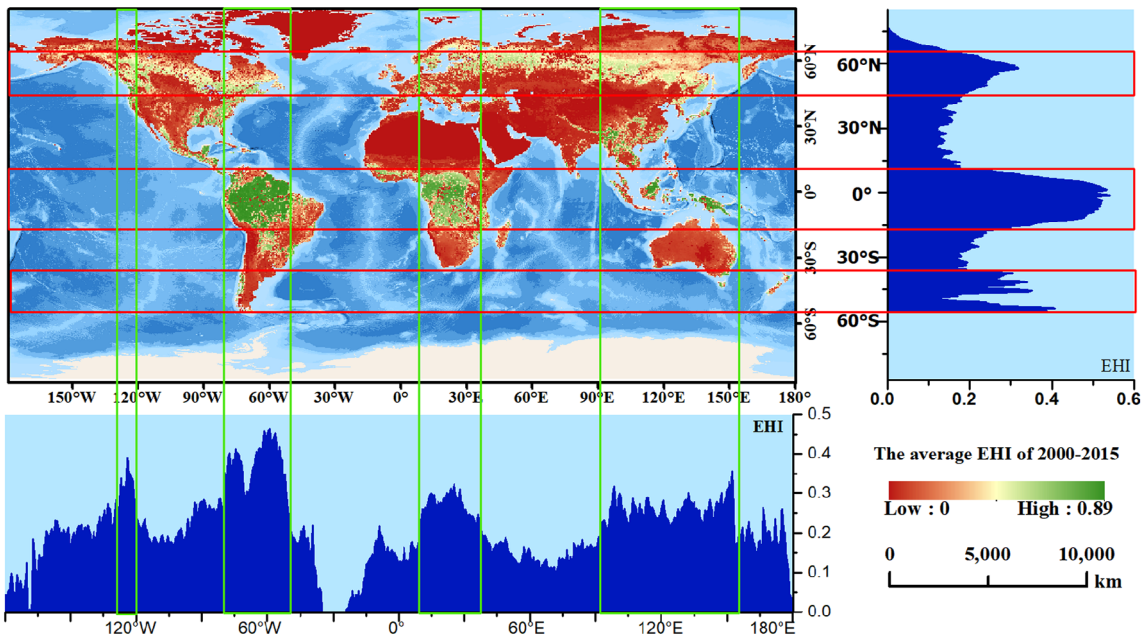

FIGURE 3 Spatial distribution of different latitude and longitude average ecosystem health index from 2000 to 2015 [Colour figure can be viewed at wileyonlinelibrary.com]

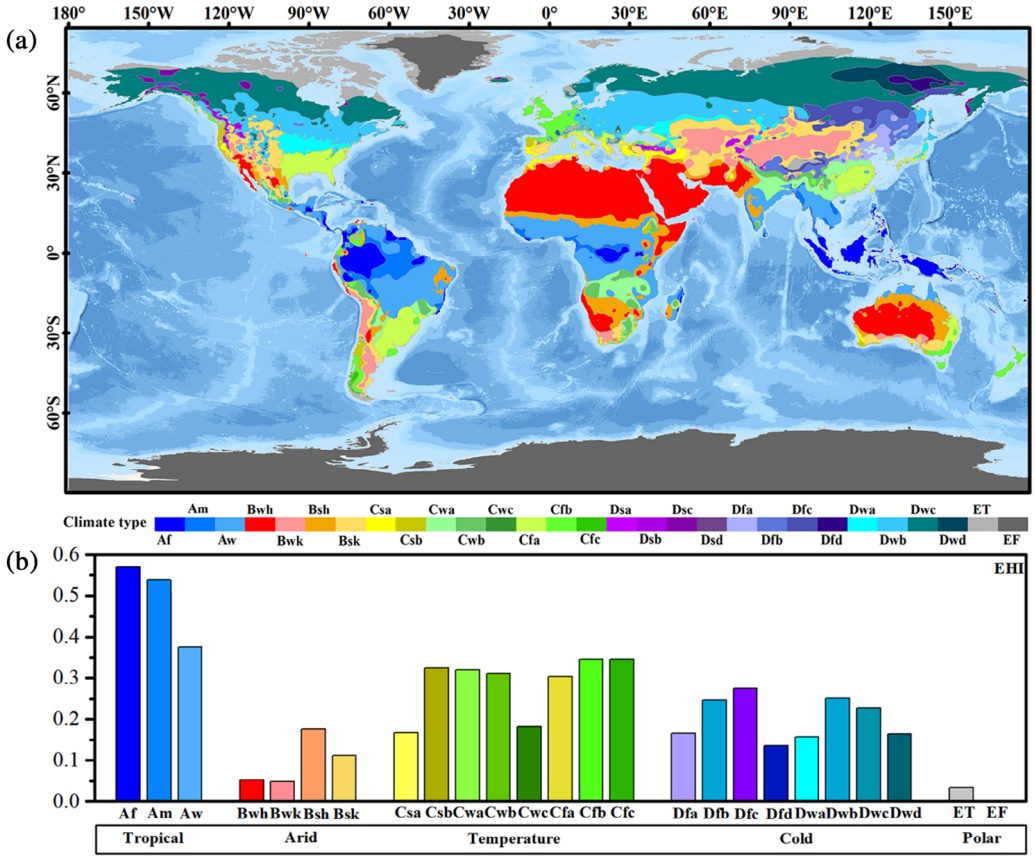

FIGURE 4 Spatial distribution of different climatic zones average ecosystem health index [Colour figure can be viewed at wileyonlinelibrary.com]

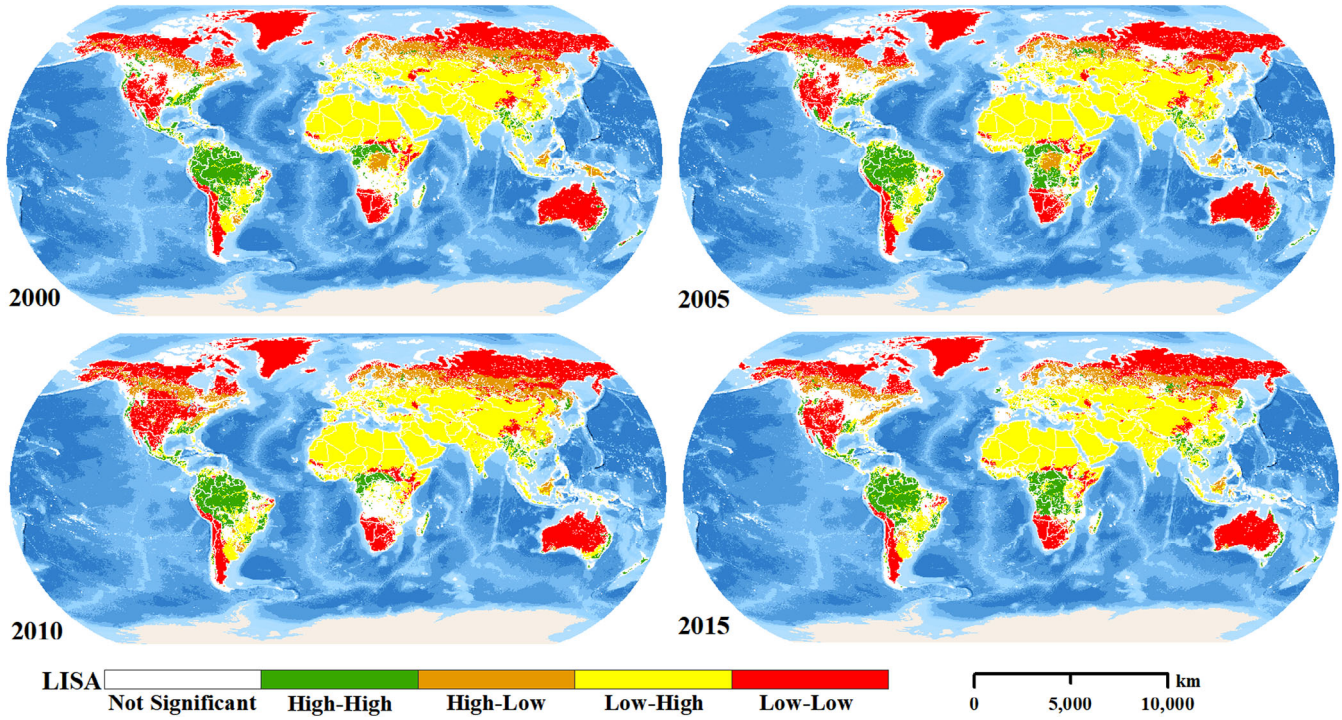

FIGURE 5 The different clustering patterns of global ecosystem health index [Colour figure can be viewed at wileyonlinelibrary.com]

of the ice sheet and plateau climate (EF) region. In this climatic zone, monthly mean temperature is below 0°C, snow is present year-round and average EHI is almost zero.

3.4 | Spatial auto-correlation analysis

The role of spatial auto-correlation is to show that the obtained distribution of global ecosystem health is not a random distribution, but a certain rule. When the Moran *I* index is positive, there is a significant positive correlation. Similar observations (high or low) tend to spatially agglomerate. The values of Moran's *I* in the study area from 2000 to 2015 are all greater than 0: 0.079, 0.069, 0.084, and 0.096, indicating that distribution of the global EHI has a certain spatial correlation and aggregation. *Z* scores are between 30 and 50. Considering that the value of Moran's *I* index is positive, we may conclude that the result is distributed at the right end of the normal distribution, which is the aggregation type. *p* value is 0, indicating that the result is not a random data generation, and the result is reliable.

Based on the calculation of global Moran's *I* index, we know that the distribution of the global EHI is clustered. Local spatial auto-correlation shows that the spatial clustering of global ecosystem health from 2000 to 2015 has a similar distribution pattern (Figure 5). The high-high clustering pattern is mainly distributed in the tropical zone, and the low-low clustering pattern is mainly distributed in the tropical desert climate zone and the polar climate zone.

3.5 | Influencing factor analysis

3.5.1 | Single factor correlation analysis

Through analysis of the Pearson correlation coefficient, the influence of a single factor on EHI change at the global and climatic zone levels can be determined. As shown in the correlation coefficient diagram (Figure 6), blue indicates a positive correlation, pink indicates a negative correlation, and the colour shade indicates the degree of correlation. Whether at the global or climatic zone level, annual average precipitation has a significant positive impact on EHI, indicating that it is the root cause of ecosystem health changes. Soil moisture has a negative impact on ecosystem health in the polar climate zone, and a positive impact in the rest of the world. Note that average annual precipitation dominates the regional differences in global ecosystem health, and its correlation with the EHI is 0.547. In addition, soil moisture is the second leading factor affecting global ecosystem health, with a correlation coefficient of 0.399.

Note that in the polar climate zone, the main factors affecting ecosystem health are annual average temperature and population

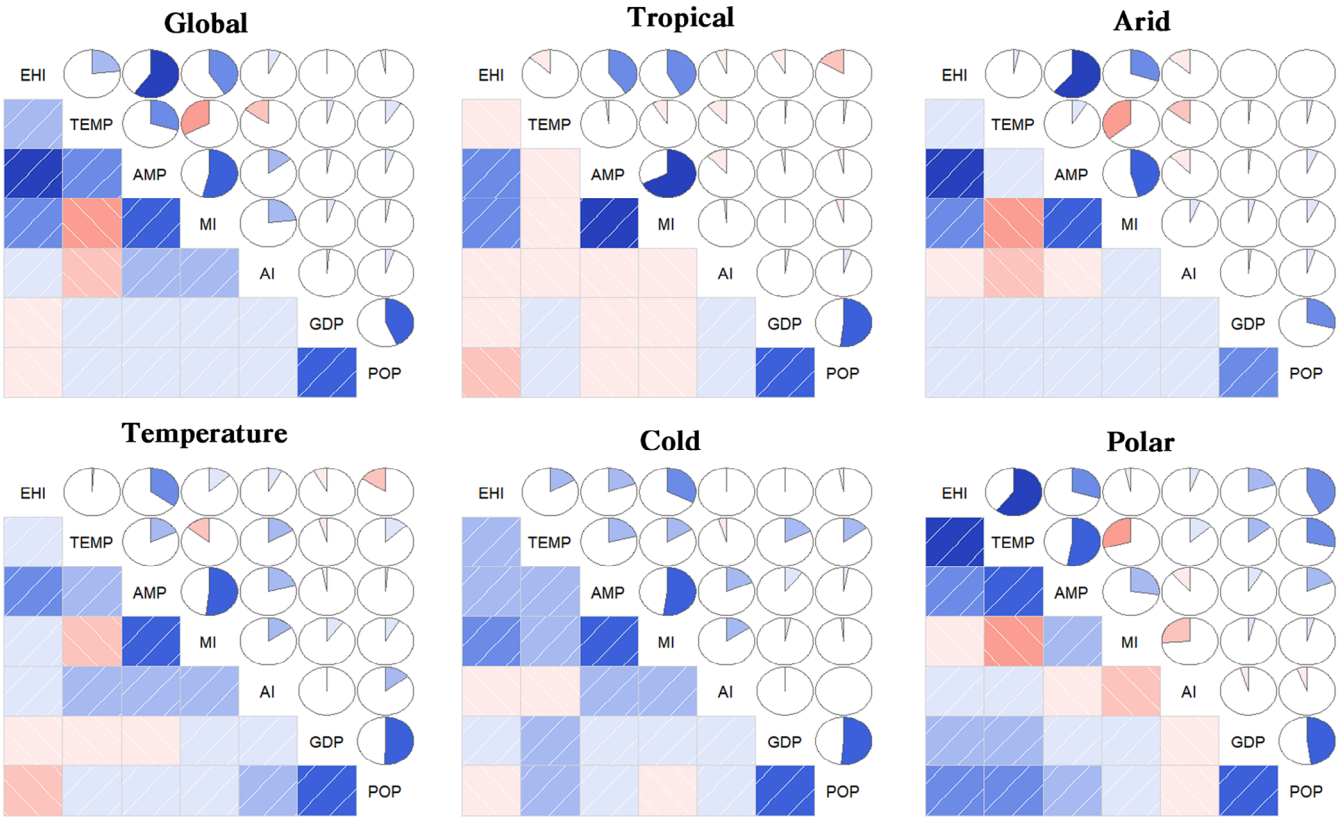

FIGURE 6 Correlation coefficient diagram of influencing factors of different climatic zones [Colour figure can be viewed at wileyonlinelibrary.com]

TABLE 3 Correlation coefficient table of influencing factors of different climatic zones

Layer	TEMP	AMP	MI	AI	GDP	POP
Global	0.264**	0.574**	0.399**	0.047**	0.074**	−0.112**
Tropical	−0.169**	0.52**	0.497**	−0.067**	−0.487**	−0.447**
Arid	−0.009**	0.68**	0.303**	−0.232**	0.109**	−0.122**
Temperature	−0.011**	0.366**	0.163**	0.072**	−0.186**	−0.191**
Cold	0.133**	0.252**	0.301**	0.004**	−0.075**	0.041**
Polar	0.674**	0.272**	−0.14**	0.244**	0.239**	0.586**

**At 0.05 level.

TABLE 4 Table of interactive influence coefficients of different climatic zones

	TEMP	AMP	MI	AI	GDP	POP	1	2	3	4
Global	0.148	0.286	0.165	0.014	0.002	0.010	TEMP ∩ AMP	TEMP ∩ MI	AMP ∩ MI	AMP ∩ POP
							0.393bi	0.382nonlinear	0.351bi	0.325nonlinear
Arid	0.036	0.052	0.069	0.029	0.013	0.016	AMP ∩ POP	TEMP ∩ MI	AMP ∩ AI	TEMP ∩ AMP
							0.331bi	0.201bi	0.204bi	0.204bi
Tropical	0.063	0.160	0.160	0.041	0.050	0.171	TEMP ∩ AMP	TEMP ∩ MI	AMP ∩ AI	MI ∩ AI
							0.10nonlinear	0.13nonlinear	0.10nonlinear	0.12nonlinear
Temperature	0.049	0.120	0.022	0.021	0.025	0.061	TEMP ∩ AMP	TEMP ∩ POP	AMP ∩ MI	AMP ∩ POP
							0.201nonlinear	0.158nonlinear	0.138bi	0.216nonlinear
Cold	0.113	0.013	0.097	0.007	0.004	0.007	TEMP ∩ AMP	TEMP ∩ MI	TEMP ∩ AI	TEMP ∩ GDP
							0.151nonlinear	0.20bi	0.149nonlinear	0.135nonlinear
Polar	0.612	0.048	0.140	0.046	0.135	0.366	TEMP ∩ AMP	TEMP ∩ MI	AMP ∩ AI	AMP ∩ POP
							0.658bi	0.745bi	0.655bi	0.688bi

Notes: Nonlinear enhanced [$q(X1 \cap X2) > q(X1)] + q(X2)$), bi-enhanced [$q(X1 \cap X2)] > \text{Max}[q(X1), q(X2)]$.

density (Table 3), whose correlation with the EHI is 0.674 and 0.586, respectively. The polar climate zone in this study is mainly tundra climate zone, mainly distributed at the northern edge of North America and Eurasia, along the coast of Greenland and in the Arctic. On some islands, the residents are mainly Eskimos, also known as Inuit. We speculate that in this extremely cold region, if temperature and population density increase slightly, ecosystem health will improve.

3.5.2 | Interactive detection analysis

Through interaction analysis of GDM, we observe that the interaction between driving factors has a significant two-way enhancement or nonlinear enhancement of ecosystem health. This shows that interaction between influencing factors has greater impact than the individual or cumulative effect of two independent factors. In accordance with the results of the interaction detector, we list the top four major interactions, all with a significance level of explanatory power of 1%.

From the global perspective (Table 4), the interaction between annual average temperature and annual average precipitation has the greatest explanatory power for the regional differences in global ecosystem health, which shows double-factor enhancement, with a q statistic of 39.3%. From the climatic zone perspective (Table 4), in tropical regions, where ecosystems are relatively healthy, the interaction between meteorological factors and socioeconomics is greater than the impact of individual factors on ecosystem health changes. For example, the interaction between annual average precipitation and population density in the tropics (43.1%) is the dominant factor affecting ecosystem health change in the region. In the warm temperate zone and cold temperate zone, where ecosystem health is at a moderate level, the interaction between the two meteorological factors is the main cause of ecosystem health change. That is, the interaction between annual mean temperature and average annual precipitation explains 20.1 and 15.1% of health changes, respectively. In the arid climatic zone, where ecosystem health is at a low to medium level, the interaction of the two meteorological factors is found to be the main cause of changes in ecosystem health. In the polar climatic zone, where ecosystem health is low, the interaction between the two meteorological factors shows great significance; the interpretive power of interaction between the two climatic factors is as high as 74.5%, and the explanatory power of the interaction between climate and socioeconomic factors (annual average precipitation and population density) is as high as 68.8%.

In addition, when a factor exists independently, it has little influence on ecosystem health, but its interaction with social and economic factors (GDP and population density) leads to significant linear or nonlinear enhancement. This shows that socioeconomic factors act as a bridge linking and strengthening other drivers in these regions.

4 | DISCUSSION

4.1 | Spatial distribution characteristics and causes of EHI

Combined with the spatial distribution pattern of ecosystem health in different longitude and latitude (Figure 3) and climatic zones (Figure 4), it can be seen that ecosystem health is significantly affected by climatic and hydrological conditions (Chen et al., 2019; Yang et al., 2019), because the regions with high value of global ecosystem health belong to the tropical rainforest climate and have abundant rainfall, which is the major and largest tropical rainforest region in the world. In addition, ecosystem health also showed high values in areas with high vegetation coverage, such as the plains of Eastern Europe, the Atlantic coastal plains and the Yunnan-Guizhou Plateau. The low-value areas of ecosystem health are mainly distributed in arid and cold regions, where the climate is arid and precipitation is scarce, and most vegetation types belong to desert steppe, such as the Qinghai-Tibet Plateau and the Sahara Desert.

4.2 | Difference analysis of driving factors

Based on an analysis of the driving factors affecting ecosystem health, global average annual precipitation and soil moisture are established as the leading factors affecting the regional heterogeneity of ecosystem health, this result is evident in Table 3 and Figure 6. He et al. (2019) explored the regional differences and influencing factors of ecosystem health in China and conclude that soil moisture is the main factor influencing the regional heterogeneity of ecosystem health in China. Similar studies show that climate influences delivery of ES (Bai, Ochuodho, & Yang, 2019; Lorencová, Harmáčková, Landová, Pártl, & Vačkář, 2016; Zhang et al., 2018), it is the main determinant of regional ecological sensitivity (Zhang & Xu, 2017). In addition, the interaction between driving factors also produces different effects, as shown in Table 4, the interaction between climate factors is usually greater than the influence of a single driving factor. However, the spatial heterogeneity of the driving factors and the interaction between driving factors on ecosystem health are often ignored in the research process. Our research shows that there is synergy among meteorological factors and socioeconomic factors, and that the dominance of driving factors differs by region.

4.3 | Characteristics and applicability of the VORS model

The VORS model used here evolved from the VOR model proposed by Costanza (2012). Many researchers on ecosystem health continue to use the more widely accepted classical vigour-organization-resilience model (Jian et al., 2015; Xue, Wang, & Niu, 2013; Yu et al., 2013). Later, the index of ES was added and evolved into the VORS model. Based on an analysis of temporal–spatial change of each index of ecosystem health (Figure 1), we can see that the fluctuation of each index of ecosystem health is relatively gentle across time, and the change trend of the EHI is relatively consistent with the change trend of EV. Combined with the spatial correlation diagram of each index of ecosystem health (Figure 7), note that the correlation

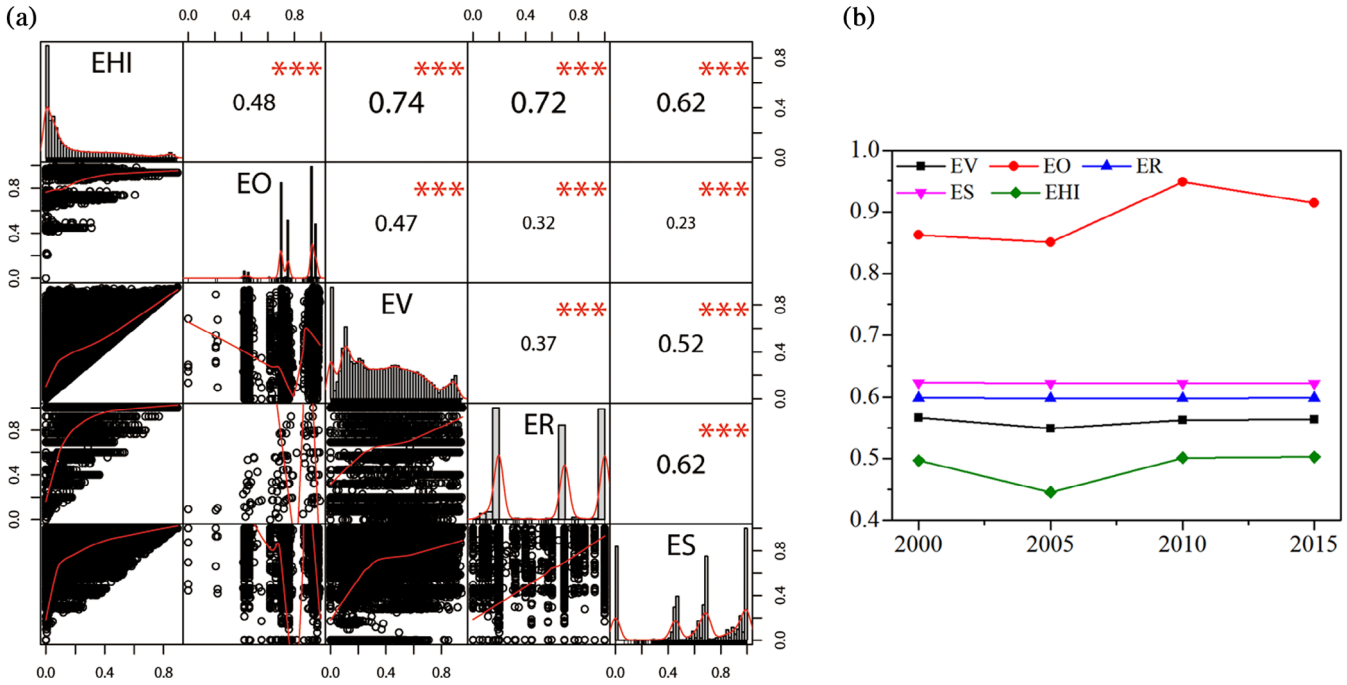

FIGURE 7 The diagram of the correlation and temporal changes of each ecosystem health indicators [Colour figure can be viewed at wileyonlinelibrary.com]

between EV and ecosystem health is greatest. Some studies show that spatial differences in ecosystem health are affected mainly by EV and ES (Yan et al., 2016). It is of great importance to introduce ES into EHA and improve the overall ecosystem assessment. Some studies show that EV is the leading factor behind spatial difference and temporal change in urban-scale ecosystem health (Peng et al., 2017). In addition, other studies show that spatial distribution of ecosystem health depends mainly on EV and ER (Shen, Shi, Zheng, & Ding, 2016). There is a positive correlation between every ecosystem health indicator and ecosystem health, and the correlation between EV and ecosystem health is greatest. In addition, there is a significant synergistic relationship among indicators, showing that they not only play a role in promoting ecosystem health but also complement each other.

Through correlation analysis of the EHI and ecosystem health indicators (VORS), we may conclude that the global ecosystem health is best matched with EV and ER (Figure 7). Thus, the question is whether it is necessary to include one or more new indicators in the widely used VOR and VORS models for various targets at different regional scales, so as to make assessment of ecosystem health more accurate and more universal.

4.4 | Uncertainty analysis

EV, EO, ER, and ES are important indicators in assessing ecosystem health. These indicators directly affect the assessment results for ecosystem health. The weights of various indicators in this study are determined mainly by referring to the existing literature and connecting with the actual situation. In addition, using the geographic detector to quantify the interaction between driving factors and their impact on ecosystem health, we found that different classification methods have particular impacts on the obtained results when the quantized driving factors are discretized. However, there is no clear standard for the method used to discretize continuous variables.

Although this study has some limitations in data acquisition and the method used, we nevertheless believe that this study is meaningful. Although the weight determination of each index is not perfect, it is by no means arbitrary as it stems from consulting a large number of studies. A geographic detector is a set of statistical methods that explores spatial variability, revealing the driving forces behind it. The detector can detect both the largest driving forces behind global ecosystem health (the independent variable corresponding to the maximum q value) and the local driving forces in different regions.

This paper's results can help researchers understand the spatial patterns of ecosystem health changes and their influencing factors, and provide scientific support for the formulation of regional ecological protection and restoration policies.

5 | CONCLUSIONS

Based on the VORS model, this study makes a preliminary diagnosis of global ecosystem health, and uses a geographic detector to detect key impact factors at the global level and at climatic zone level, as well as the impact of the interaction between each factor on ecosystem health. The main conclusions are as follows:

1. Between 2000 and 2015, the environmentally healthier countries of the world accounted for more than 50% of the total number, but they accounted for far less than 50% of the total area.
2. Ecosystem health distribution is based on latitude and longitude. There are seven critical zones, with low latitudinal distribution for three zones (13°N–18°S, 45°N–65°N, 35°S–56°S), and longitudinal distribution for two critical zones in each of the Eastern and Western hemispheres (47°W–80°W, 120°W–130°W, 8°E–37°E, 92°E–157°E). The intersection of these critical zones with high levels of ecosystem health occurs mainly in the north of East Africa, South America, Southeast Asia, and so on.
3. The global EHI has a similar spatial distribution pattern, and the EHI in the tropics near the equator (0°N–13°N, 0°S–18°S) is higher than of all other climatic zones.
4. Annual average rainfall (r^2 = .574) and soil moisture (r^2 = .399) are the main factors influencing ecosystem health. Socioeconomic factors act as bridges, linking and reinforcing the influence of other factors in areas with medium to low levels of ecosystem health.

ACKNOWLEDGMENTS

This research work was supported jointly by the Strategic Priority Research Program of the Chinese Academy of Sciences (No. XDA23060100), National Key Research Program of China (No. 2016YFC0502300 & No. 2016YFC0502102), Western Light Talent Program (Category A) (No. 2018-99), United Fund of Karst Science Research Center (No. U1612441), Science and Technology Plan of Guizhou Province of China (No. 2017-2966).

CONFLICT OF INTEREST

The authors declare that there is no conflict of interest.

DATA AVAILABILITY STATEMENT

Author elects to not share data.

ORCID

Xiaoyong Bai https://orcid.org/0000-0001-9705-5574

REFERENCES

Ainslie, W. B. (1994). Rapid wetland functional assessment: Its role and utility in the regulatory arena. *Water Air & Soil Pollution*, *77*(3–4), 237–248. https://doi.org/10.1007/BF00478431

Anselin, L. (1995). Local indicators of spatial association—LISA. *Geographical Analysis*, *27*, 93–115. https://doi.org/10.1111/j.1538-4632.1995.tb00338.x

Bai, Y., Ochuodho, T. O., & Yang, J. (2019). Impact of land use and climate change on water-related ecosystem services in Kentucky, USA. *Ecological Indicators*, *102*, 51–64. https://doi.org/10.1016/j.ecolind.2019.01.079

Bingkui, Q., Huilei, L., Min, Z., & Lu, Z. (2015). Vulnerability of ecosystem services provisioning to urbanization: A case of China. *Ecological Indicators*, *57*, 505–513. https://doi.org/10.1016/j.ecolind.2015.04.025

Chen, C., Park, T., Wang, X., Piao, S., Xu, B., Chaturvedi, R. K., … Myneni, R. B. (2019). China and India lead in greening of the world through land-use management. *Nature Sustainability*, *2*, 122–129. https://doi.org/10.1038/s41893-019-0220-7

Cheng, X., Chen, L., Sun, R., & Kong, P. (2018). Land use changes and socio-economic development strongly deteriorate river ecosystem health in one of the largest basins in China. *Science of the Total Environment*, *616–617*, 376–385. https://doi.org/10.1016/j.scitotenv.2017.10.316

Colding, J. (2007). 'Ecological land-use complementation' for building resilience in urban ecosystems. *Landscape and Urban Planning*, *81*(1–2), 46–55. https://doi.org/10.1016/j.landurbplan.2006.10.016

Costanza, R. (1992a). Towards an operational definition of health. In R. Costanza, B. Norton, & B. D. Haskell (Eds.), *Ecosystem health—New goals for ecosystem management* (pp. 239–256). Washington, DC: Island Press. http://hdl.handle.net/1969.3/25412

Costanza, R. (1992b). Toward an operational definition of ecosystem health. In *Ecosystem health: New goals for environmental management*, Washington, DC: Island Press. https://doi.org/10.2307/2136932

Costanza, R. (2012). Ecosystem health and ecological engineering. *Ecological Engineering*, *45*(8), 24–29. https://doi.org/10.1016/j.ecoleng.2012.03.023

Costanza, R., & Mageau, M. (1999). What is a healthy ecosystem? *Aquatic Ecology*, *33*(1), 105–115. https://doi.org/10.1023/A:1009930313242

Costanza, R., Mageau, M., Norton, B., & Patten, B. C. (1998). Predictors of ecosystem health. In D. J. Rapport, R. Costanza, P. Epstein, C. Gaudet, & R. Levins (Eds.), *Ecosystem health* (pp. 140–250). Malden, MA: Blackwell Science. https://doi.org/10.1017/S1466046600000612

Deng, Y., Wang, S., Bai, X., Luo, G., Wu, L., Cao, Y., … Tian, S. (2019). Variation trend of global soil moisture and its cause analysis. *Ecological Indicators*, *110*, 105939. https://doi.org/10.1016/j.ecolind.2019.105939

Dobbs, C., Escobedo, F. J., & Zipperer, W. C. (2011). A framework for developing urban forest ecosystem services and goods indicators. *Landscape and Urban Planning*, *99*(3–4), 196–206. https://doi.org/10.1016/j.landurbplan.2010.11.004

Frondoni, R., Mollo, B., & Capotorti, G. (2011). A landscape analysis of land cover change in the Municipality of Rome (Italy): Spatio-temporal characteristics and ecological implications of land cover transitions from 1954 to 2001. *Landscape and Urban Planning*, *100*(1–2), 117–128. https://doi.org/10.1016/j.landurbplan.2010.12.002

He, J., Pan, Z., Liu, D., & Guo, X. (2019). Exploring the regional differences of ecosystem health and its driving factors in China. *Science of the Total Environment*, *673*, 553–564. https://doi.org/10.1016/j.scitotenv.2019.03.465

Howell, P. E., Muths, E., Hossack, B. R., Sigafus, B. H., & Chandler, R. B. (2018). Increasing connectivity between metapopulation ecology and landscape ecology. *Ecology*, *99*, 99–1128. https://doi.org/10.1002/ecy.2189

Ishtiaque, A., Myint, S. W., & Wang, C. (2016). Examining the ecosystem health and sustainability of the world's largest mangrove forest using multi-temporal MODIS products. *Science of the Total Environment*, *569–570*, 1241–1254. https://doi.org/10.1016/j.scitotenv.2016.06.200

Jian, P., Yanxu, L., Jiansheng, W., Huiling, L., & Xiaoxu, H. (2015). Linking ecosystem services and landscape patterns to assess urban ecosystem health: A case study in Shenzhen City, China. *Landscape and Urban Planning*, *143*, 56–68. https://doi.org/10.1016/j.landurbplan.2015.06.007

Kang, P., Chen, W., Hou, Y., & Li, Y. (2018). Linking ecosystem services and ecosystem health to ecological risk assessment: A case study of the Beijing-Tianjin-Hebei urban agglomeration. *Science of the Total Environment*, *636*, 1442–1454. https://doi.org/10.1016/j.scitotenv.2018.04.427

Lavorel, S., Grigulis, K., Leitinger, G., Kohler, M., Schirpke, U., & Tappeiner, U. (2017). Historical trajectories in land use pattern and grassland ecosystem services in two European alpine landscapes. *Regional Environmental Change*, *17*(8), 2251–2264. https://doi.org/10.1007/s10113-017-1207-4

Li, Q., Wang, S. J., Bai, X. Y., Luo, G., Song, X., Tian, Y., … Tian, S. (2020). Change detection of soil formation rate in space and time based on multi source data and geospatial analysis techniques. *Remote Sensing*, *12*(1), 121. https://doi.org/10.3390/rs12010121

Liao, C., Yue, Y., Wang, K., Fensholt, R., Tong, X., & Brandt, M. (2018). Ecological restoration enhances ecosystem health in the karst regions of southwest China. *Ecological Indicators*, *90*, 416–425. https://doi.org/10.1016/j.ecolind.2018.03.036

Lorencová, E. K., Harmáčková, Z. V., Landová, L., Pártl, A., & Vačkář, D. (2016). Assessing impact of land use and climate change on regulating ecosystem services in The Czech Republic. *Ecosystem Health & Sustainability*, *2*(3). https://doi.org/10.1002/ehs2.1210

Lu, F., & Li, Z. (2003). A model of ecosystem health and its application. *Ecological Modelling*, *170*, 55–59. https://doi.org/10.1016/S0304-3800(03)00300-4

Mageau, M. T., Costanza, R., & Ulancowicz, R. E. (1995). The development and initial testing of a quantitative assessment of ecosystem health. *Ecosystem Health*, *1*, 201–213. https://doi.org/10.1111/j.1600-0447.1960.tb09475.x

Mariano, D. A., Santos, C. A. C. D., Wardlow, B. D., Anderson, M. C., Schiltmeyer, A. V., Tadesse, T., & Svoboda, M. D. (2018). Use of remote sensing indicators to assess effects of drought and human-induced land degradation on ecosystem health in northeastern Brazil. *Remote Sensing of Environment*, *213*, 129–143. https://doi.org/10.1016/j.rse.2018.04.048

Marulli, J., & Mallarach, J. M. (2005). A GIS methodology for assessing ecological connectivity: Application to the Barcelona metropolitan area. *Landscape and Urban Planning*, *71*(2–4), 243–262. https://doi.org/10.1016/s0169-2046(04)00079-9

Moran, P. A. P. (1950). Notes on continuous stochastic phenomena. *Biometrika*, *37*(1–2), 17–23. https://doi.org/10.2307/2332142

Munavar, Z., Carsten, M., Christian, H., Dietrich, D., & Nicole, W. M. (2018). Assessment of vegetation degradation in mountainous pastures of the Western Tien-Shan, Kyrgyzstan, using EMODIS NDVI. *Ecological Indicators*, *95*, 527–543. https://doi.org/10.1016/j.ecolind.2018.07.060

Pantus, F. J., & Dennision, W. (2005). Quantifying and evaluating ecosystem health: A case study from Moreton Bay, Australia. *Environmental Management.*, *36*(5), 757–771. https://doi.org/10.1007/s00267-003-0110-6

Peng, J., Liu, Y. X., Li, T. Y., & Wu, J. S. (2017). Regional ecosystem health response to rural land use change: A case study in Lijiang City, China. *Ecological Indicators*, *72*, 399–410. https://doi.org/10.1016/j.ecolind.2016.08.024

Peng, J., Wang, Y. L., Wu, J. S., Shen, H., & Pan, Y. J. (2011). Research progress on evaluation frameworks of regional ecological sustainability. *Chinese Geographical Science*, *21*(4), 496–510. https://doi.org/10.1007/s11769-011-0490-0

Peng, W. F., Kuang, T. T., & Tao, S. (2019). Quantifying influences of natural factors on vegetation NDVI changes based on geographical detector in Sichuan, western China. *Journal of Cleaner Production*, *233*, 353–367. https://doi.org/10.1016/j.jclepro.2019.05.355

Rapport, D. J. (1989). What constitutes ecosystem health? *Perspectives in Biology and Medicine*, *33*(1), 120–132. https://doi.org/10.1353/pbm.1990.0004

Rapport, D. J. (2007). Sustainability science: An ecohealth perspective. *Sustainability Science*, *2*(1), 77–84. https://doi.org/10.1007/s11625-006-0016-3

Rapport, D. J., Bohm, G., Buckingham, D., Cairns, J., Costanza, R., Karr, J. R., … Whitford, W. G. (1999). Ecosystem health: The concept, the ISEH, and the important tasks ahead. *Ecosystem Health*, *5*(2), 82–90. https://doi.org/10.1046/j.1526-0992.1999.09913.x

Rapport, D. J., Costanza, R., & McMichael, A. J. (1998). Assessing ecosystem health. *Trends in Ecology & Evolution.*, *13*(10), 397–402. https://doi.org/10.1016/S0169-5347(98)01449-9

Rapport, D. J., & Hildén, M. (2013). An evolving role for ecological indicators: From documenting ecological conditions to monitoring drivers and policy responses. *Ecological Indicators*, *28*, 10–15. https://doi.org/10.1016/j.ecolind.2012.05.015

Rombouts, I., Beaugrand, G., Artigas, L. F., Dauvin, J. C., Gevaert, F., Goberville, E., … Kirby, R. R. (2013). Evaluating marine ecosystem health: Case studies of indicators using direct observations and modelling methods. *Ecological Indicators*, *24*, 353–365. https://doi.org/10.1016/j.ecolind.2012.07.001

Shen, C. C., Shi, H. H., Zheng, W., & Ding, D. W. (2016). Spatial heterogeneity of ecosystem health and its sensitivity to pressure in the waters of a nearshore archipelago. *Ecological Indicators*, *61*, 822–832. https://doi.org/10.1016/j.ecolind.2015.10.035

Song, D. B., Gao, Z. Q., Zhang, H., Xu, F. X., Zheng, X., Ai, J., … Zhang, H. (2017). GIS-based health assessment of the marine ecosystem in Laizhou Bay, China. *Marine Pollution Bulletin*, *125*(1–2), 242–249. https://doi.org/10.1016/j.marpolbul.2017.08.027

Styers, D. M., Chappelka, A. H., Marzen, L. J., & Somers, G. L. (2010). Developing a land-cover classification to select indicators of forest ecosystem health in a rapidly urbanizing landscape. *Landscape and Urban Planning*, *94*(3–4), 158–165. https://doi.org/10.1016/j.landurbplan.2009.09.006

Tang, D. H., Liu, X. J., & Zou, X. Q. (2018). An improved method for integrated ecosystem health assessments based on the structure and function of coastal ecosystems: A case study of the Jiangsu coastal area, China. *Ecological Indicators*, *84*, 82–95. https://doi.org/10.1016/j.ecolind.2017.08.031

Tian, F., Fensholt, R., Verbesselt, J., Grogan, K., Horion, S., & Wang, Y. (2015). Evaluating temporal consistency of long-term global NDVI datasets for trend analysis. *Remote Sensing of Environment*, *163*, 326–340. https://doi.org/10.1016/j.rse.2015.03.031

Wang, J. F., & Xu, C. D. (2017). Geographical detector: Principles and prospects. *Acta Geographica Sinica*, *72*(1), 116–134. https://doi.org/10.11821/dlxb201701010

Wang, P., Deng, X., Zhou, H., & Wei, Q. (2018). Responses of urban ecosystem health to precipitation extreme: A case study in Beijing and Tianjin. *Journal of Cleaner Production*, *177*, 124–133. https://doi.org/10.1016/j.jclepro.2017.12.125

Xiao, R., Liu, Y., Fei, X. F., Yu, W. X., Zhang, Z., & Meng, Q. (2019). Ecosystem health assessment: A comprehensive and detailed analysis of the case study in coastal metropolitan region, eastern China. *Ecological Indicators*, *98*, 363–376. https://doi.org/10.1016/j.ecolind.2018.11.010

Xue, P., Wang, B., & Niu, X. (2013). A simplified method for assessing forest health, with application to Chinese fir plantations in Dagang Mountain, Jiangxi, China. *Journal of Food Agriculture and Environment*, *11*(2), 1232–1238. Retrieved from https://www.researchgate.net/publication/286810926_A_simplified_method_for_assessing_forest_health_with_application_to_Chinese_fir_plantations_in_Dagang_Mountain_Jiangxi_China.

Yan, Y., Zhao, C., Wang, C., Shan, P., Zhang, Y., & Wu, G. (2016). Ecosystem health assessment of the Liao River Basin upstream region based on ecosystem services. *Acta Ecologica Sinica*, *36*(4), 294–300. https://doi.org/10.1016/j.chnaes.2016.06.005

Yang, Y. J., Song, G., & Lu, S. (2020). Assessment of land ecosystem health with Monte Carlo simulation: A case study in Qiqihaer, China. *Journal of Cleaner Production*, *250*, 119522. https://doi.org/10.1016/j.jclepro.2019.119522

Yang, Y. J., Wang, S. J., Bai, X. Y., Tan, Q., Li, Q., Wu, L., … Deng, Y. (2019). Factors affecting long-term trends in global NDVI. *Forests*, *10*, 372. https://doi.org/10.3390/f10050372

Yu, G., Yu, Q., Hu, L., Zhang, S., Fu, T., Zhou, X., … Jia, H. (2013). Ecosystem health assessment based on analysis of a land use database. *Applied Geography*, *44*, 154–164. https://doi.org/10.1016/j.apgeog.2013.07.010

Zhang, H., Fan, J., Cao, W., Zhong, H., Harris, W., Gong, G., & Zhang, Y. (2018). Changes in multiple ecosystem services between 2000 and 2013 and their driving factors in the Grazing Withdrawal Program, China. *Ecological Engineering*, *116*, 67–79. https://doi.org/10.1016/j.ecoleng.2018.02.028

Zhang, H. Q., & Xu, E. Q. (2017). An evaluation of the ecological and environmental security on China's terrestrial ecosystems. *Scientific Reports*, *7*(1), 811. https://doi.org/10.1038/s41598-017-00899-x

Zhang, J. H., Feng, Z. M., Jiang, L. G., & Yang, Y. Z. (2015). Analysis of the correlation between NDVI and climate factors in the Lancang River basin. *Journal of Natural Resources*, *30*, 1425–1435. https://doi.org/10.11849/zrzyxb.2015.09.001

Zheng, Y. T., Han, J. G., Huang, Y. F., Fassnacht, S. R., Xie, S., Lv, E., & Chen, M. (2018). Vegetation response to climate conditions based on NDVI simulations using stepwise cluster analysis for the Three-River headwaters region of China. *Ecological Indicators*, *92*, 18–29. https://doi.org/10.1016/j.ecolind.2017.06.040

How to cite this article: Ran C, Wang S, Bai X, et al. Evaluation of temporal and spatial changes of global ecosystem health. *Land Degrad Dev*. 2021;32:1500–1512. https://doi.org/10.1002/ldr.3813